

# Modeling of the polymerization and crystallization kinetic coupling of polyamide 6 synthesized from $\epsilon$ -caprolactam

Céline Vicard, Olivier De Almeida\*, Arthur Cantarel, Gérard Bernhart

*Institut Clément Ader (ICA), Université de Toulouse, CNRS, IMT Mines Albi, UPS, INSA, ISAE-SUPAERO, Campus Jarlard, 81013, Albi CT Cedex 09, France*



## HIGHLIGHTS

- Coupled polymerization and crystallization is modelled over a wide temperature range.
- An Hillier formulation is used to consider the interaction between both mechanisms.
- A corrective factor allows considering the polymerization effect on crystallization.
- Limitations of previous models from literature are analysed.

## ARTICLE INFO

### Keywords:

Coupled polymerization-crystallization model  
DSC kinetics  
Time-temperature-transformation diagram  
Liquid thermoplastic composite manufacturing  
Polyamide 6

## ABSTRACT

Optimization of polyamide 6 (PA6) composite manufacturing by liquid processes requires a better prediction of kinetics during synthesis. This study proposes a new modeling approach that considers the interaction between PA6 polymerization and crystallization over a wide temperature range (403–473 K). Different polymerization and crystallization models taken from literature were used in this study. Few attempts to describe the coupling between phenomena have been reported, and all have raised physical limitations. A new coupling equation was adapted from Hillier coupling, first introduced to model secondary crystallization of semi-crystalline thermoplastics. This equation properly predicted kinetics at high temperature when the coupling is limited. However, it failed in predicting the particular crystallization kinetics in the early stages of polymerization at low temperature, as crystallization may require that polymerized chains reach a certain length or concentration in the reactive mixture. A factor was successfully introduced in order to correct the crystallization behavior. From this new model, a wide isothermal Time-Temperature-Transformation (TTT) diagram was produced, which assists in cure path design for composite manufacturing.

## 1. Introduction

Reactive thermoplastic systems are promising alternatives to conventional thermoplastic matrices for the manufacturing of composite laminates. Contrary to high molecular weight thermoplastics, which high viscosity limits fiber impregnation rate and requires high pressure processes, the low viscosity of reactive systems make them compatible with liquid processes used for thermoset matrix composite manufacturing (Resin Transfer Molding, Liquid Resin Infusion) [1]. Thermoplastic composites made from reactive systems combine the advantages of thermoset composite processes, that offer the possibility of manufacturing large and non-uniform 3D composite parts, and thermoplastic matrix properties, which enable welding, reshaping and recycling composite parts afterwards.

Among the available reactive thermoplastic systems, polyamide 6

(PA6) synthesized by anionic ring-opening polymerization (AROP) of  $\epsilon$ -caprolactam is particularly attractive for transportation and energy applications. It offers a suitable balance between mechanical properties and material cost [1] and does not require extensive modifications of standard liquid process equipment. PA6 polymerization is achieved *in situ* during and after impregnation of composite reinforcements. The synthesis can be parametrized using various pair and ratio of catalyst and activator and controlled by temperature [1–3].

The particularity of the PA6 synthesis is that the chains polymerization and their crystallization can occur simultaneously depending on the temperature applied [4–6] and both affect the viscosity of the system. These phenomena are even coupled as the crystallization kinetics depend on the amount of polymer chains available. The understanding of the polymerization/crystallization interaction is even more critical given that their temperature dependencies are contrary. A

\* Corresponding author.

E-mail address: [olivier.dealmeida@mines-albi.fr](mailto:olivier.dealmeida@mines-albi.fr) (O. De Almeida).

high processing temperature accelerates the polymerization kinetics while disabling crystallization (which will occur during cooling). Conversely, a low temperature slows down the polymerization but facilitates crystallization; though issues due to the coupling between phenomena may appear.

Different hypotheses have been reported in the literature to explain how phenomena interact. Specifically, crystallization could not proceed right from the beginning of the reaction as a minimum concentration or a minimal length of polymerized oligomers are required for nucleation [7–10]. The crystallization could also change the concentration of reactants in the mixture, either by reducing the volume available for polymerization (increases the concentration) or by entrapping reactive species in crystals (decreases the concentration), which would have an impact on the synthesis kinetics [5,7,11–13].

As the temperature range of PA6 synthesis coincides with that of crystallization, a proper control of the reaction advancement and a prediction of final composite properties are complex yet crucial. To avoid expensive trial-and-error empirical optimization, a process simulation can be developed in order to optimize the cycle time, composite properties and dimensional stability after demolding. In particular, this requires a modeling of the synthesis kinetics including both polymerization and crystallization. This modeling also allows construction of a Time-Temperature-Transformation (TTT) diagram, which summarizes the events occurring over time at different temperatures [14]. Such diagrams represent a convenient tool for assessing a cure path and final properties of composites involving reactive matrices. From a unique diagram, different processing routes can be defined for any process while avoiding use of complex simulations.

The global heat flow  $\varphi$  [ $\text{W g}^{-1}$ ] recorded during the PA6 AROP from  $\epsilon$ -caprolactam is the sum of the polymerization heat flow  $\varphi_p$  and the crystallization heat flow  $\varphi_c$  (eq. (1)).

$$\varphi(t) = \varphi_p(t) + \varphi_c(t) \quad (1)$$

To model the evolution of  $\varphi$ , the relative degree of conversion  $\alpha$  [–] and the relative degree of crystallinity  $\beta$  [–] are generally preferred as they allow using kinetic differential equations.  $\alpha$  is defined by equation (2), where  $X_p$  [wt.%] is the mass fraction of polymerization and  $\Delta H_p^\infty$  [ $\text{J g}^{-1}$ ] is the final enthalpy of polymerization.

$$\alpha(t) = \frac{X_p(t)}{X_p^\infty} = \frac{1}{\Delta H_p^\infty} \int_0^t \varphi_p(\tau) d\tau \quad (2)$$

In the case of the PA6 synthesis, the polymerization kinetics are modeled either through a mechanistic differential equation based on chemical reaction kinetics and monomer concentration [15–20], or by using a semi-empirical equation [19,21–27]. Wittmer et al. early proposed a first-order equation with an Arrhenius temperature dependence [21]. Malkin et al. [22,24,28] improved this polymerization equation by introducing an autocatalytic reaction rate term and Camargo et al. [29] proposed to use an  $n^{\text{th}}$ -order reaction. This model has since been extensively used in the literature [13,30–35] and remains the reference.

In a similar manner, the crystallization heat flow is defined through the relative degree of crystallinity  $\beta$  [–] by equation (3), where  $X_c$  [wt.%] is the mass fraction crystallinity.

$$\beta(t) = \frac{X_c(t)}{X_c^\infty} = \frac{1}{\Delta H_c^\infty} \int_0^t \varphi_c(\tau) d\tau \quad (3)$$

In order to model the crystallization during the PA6 synthesis, the literature proposed to use models describing bulk polymer crystallization, such as the Avrami-Kolmogorov model [23,33]. Malkin et al. [24,36–39] have proposed a new differential equation to describe either bulk polymer crystallization and PA6 crystallization during synthesis. This model includes an autocatalytic term improving the kinetic prediction at the end of crystallization.

To model the coupling behavior between polymerization and crystallization, different levels of interaction have been considered in the

literature. A recent study [40] proposed to use a simple sum (eq. (4)), considering that both transformations are independent. The total heat flow of reaction  $\varphi$  is calculated from  $\varphi_p^\infty$  and  $\varphi_c^\infty$  [ $\text{W g}^{-1}$ ], that refer respectively to the final heat of polymerization and crystallization of the system at the end of the reaction, and from the degree of conversion  $\alpha$  and the degree of crystallinity  $\beta$ . This approach is however not valid from a physical point of view as crystallization necessarily depends on the availability of polymerized chains.

$$\varphi(t) = \varphi_p^\infty \frac{d\alpha}{dt} + \varphi_c^\infty \frac{d\beta}{dt} \quad (4)$$

In the literature [13,41], the most used coupling equation has been proposed by Malkin and Bolgov (eq. (5)). The term  $B$  [–] has been defined in this study as the degree of crystallinity within the reactive mixture. It differs from the relative degree of crystallinity of equation (3) that corresponds to the crystallization of the bulk polymer. Although if no coupling with polymerization is considered, then  $B = \beta$ .

In equation (5), the crystallization kinetics  $\dot{\beta}$  are proportional to the degree of conversion  $\alpha$  at any time and both phenomena are initiated simultaneously with temperature. It thus assumes that crystallization can occur right from the beginning of the reaction, even when the system only consists of monomers and oligomers. Moreover, the crystallization kinetics of a newly synthesized chain is assumed to be only dependent on the time elapsed since the beginning of the reaction, with no consideration to the moment it was actually formed. These assumptions induce issues with the applicability of the Malkin coupling equation.

$$\varphi(t) = \varphi_p^\infty \frac{d\alpha}{dt} + \varphi_c^\infty \frac{d\beta}{dt} \alpha(t) \quad (5)$$

The aim of this study is to investigate the limitations of the Malkin coupling model and to overcome them by proposing a new coupling equation. Models are based on a previous experimental study of the PA6 AROP from  $\epsilon$ -caprolactam [10]. The reaction kinetics were directly identified using calorimetric method (DSC), contrary to most of the literature dealing with this synthesis, which are based on temperature measurements in an adiabatic reactor. DSC results could be directly used for the identification of kinetic models.

The polymerization kinetic model was identified on this experimental database and complementary experiments of crystallization from the melt were achieved in order to define an appropriate crystallization model. The results obtained with the Malkin coupling model are then compared and a new coupling equation is presented. It was adapted from a kinetic coupling developed by Hillier to model the crystallization of bulk polymers when they exhibit a secondary crystallization [42]. After presenting the coupling formulation, the accuracy of the model to predict the total heat flow over time and its coherence with physical phenomena are discussed. Finally, an isothermal TTT diagram of the PA6 synthesis was built based on the model proposed, gathering both polymerization and crystallization evolutions.

## 2. Experimental

### 2.1. Synthesis kinetics and coupling behavior

The modeling of PA6 synthesis was based on experimental data detailed in Ref. [10]. In this previous study, PA6 was synthesized by anionic ring-opening polymerization from  $\epsilon$ -caprolactam with products supplied by Brüggemann Chemical, Germany. The products used for PA6 polymerization were the  $\epsilon$ -caprolactam monomer “AP-Nylon”, caprolactam magnesium bromide as catalyst ( $\text{MgBrCl}$  - “Nyrin C1” 1.4 mol  $\text{kg}^{-1}$  in caprolactam) and bifunctional hexamethylene-1,6-dicarbamoylactam as activator (HDCL - “Brüggolen C20P” 2.0 mol  $\text{kg}^{-1}$  in caprolactam). Syntheses were achieved with a reactive mixture

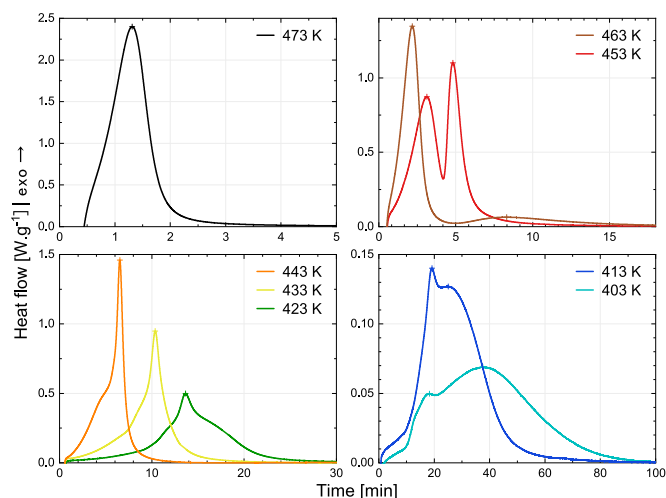


Fig. 1. PA6 global synthesis kinetics  $\dot{\gamma}$  measured in isothermal conditions with DSC.

which MgBrCL/HDCL ratio was 0.79/1.10 mol.% of CL.

The global heat flow  $\phi$  [W g<sup>-1</sup>] released during synthesis was recorded by DSC at various temperatures between 403 and 473 K (Fig. 1) and heating rates. The degree of global transformation  $\gamma$  [–] was defined by equation (6), where  $Q_{tot}$  [J g<sup>-1</sup>] is the total heat of reaction (both polymerization and crystallization). The global synthesis kinetics  $\dot{\gamma}$  [s<sup>-1</sup>] are obtained from the temporal derivative of the degree of global transformation  $\gamma$ .

$$\gamma(t) = \frac{1}{Q_{tot}} \int_0^t \phi(\tau) d\tau \quad (6)$$

The DSC curves and data recorded by TGA, DSC and WAXS on polymerized samples were used to quantify the total heat of reaction  $Q_{tot}$  [J g<sup>-1</sup>], the degree of conversion  $X_p^\infty$  [wt.%] and the crystallization enthalpy  $\Delta H_c$  [J g<sup>-1</sup>] for each isothermal synthesis temperature (Table 1). The theoretical total enthalpy of polymerization  $\Delta H_p^{100\%}$  was also calculated and estimated as  $123.5 \pm 4.1$  J g<sup>-1</sup>.

From the analysis of this experimental dataset, specific behaviors of the coupling between polymerization and crystallization have been identified. When the PA6 synthesis is achieved at high temperature, i.e. above 473 K, the low supercooling prevents the crystallization to occur and the synthesis only depends on the polymerization kinetics. The crystalline structure is formed afterward during the cooling and the final PA6 properties are similar to a standard PA6. At lower synthesis temperature, the polymerization kinetics are reduced and the higher degree of supercooling activates the crystallization in a second stage of the synthesis. Below 433 K, the crystallization kinetics strongly depend on the kinetics of chain extension and the polymerization thus controls the overall synthesis time.

Table 1

Total heat of reaction, mass fraction of polymerization and crystallization enthalpy measured during the PA6 synthesis at different isothermal temperatures.

Synthesis temperature	Total heat of reaction	Mass fraction of polymerization	Crystallization enthalpy
$T_{iso}$ [K]	$Q_{tot}$ [J g <sup>-1</sup> ]	$X_p^\infty$ [wt.%]	$\Delta H_c$ [J g <sup>-1</sup> ]
403	196.3 ± 11.1	91.8 ± 0.1	82.8 ± 11.8
413	205.6 ± 14.5	93.8 ± 0.6	90.3 ± 15.1
423	219.8 ± 3.3	94.3 ± 1.2	102.3 ± 5.2
433	211.9 ± 1.8	94.8 ± 0.5	95.2 ± 4.4
443	198.4 ± 8.3	94.9 ± 1.1	80.3 ± 9.2
453	194.7 ± 6.3	96.7 ± 0.1	75.1 ± 7.5
463	142.3 ± 10.1	95.8 ± 0.6	24.0 ± 10.9
473	121.7 ± 4.5	94.6 ± 0.7	4.3 ± 6.0

The previous results also highlighted that a high degree of crystallinity and a thick lamellar morphology are obtained when crystallization occurs simultaneously with polymerization, probably due to a higher mobility of polymer chains within the monomer medium. Finally, at low temperature, it was observed that crystallization does not start at the early stage of the synthesis. This was explained by the fact that nucleation requires a minimal chain length [7,8,43,44] or a minimal concentration of oligomers [7,9] to proceed.

## 2.2. Isothermal crystallization from the melt

The experimental study in Ref. [10] was completed with a DSC crystallization from the melt campaign performed on a PA6 sample synthesized at  $T_{iso} = 423$  K. Tests were conducted with a power-compensated PerkinElmer 8500 DSC under nitrogen on 9–12 mg samples sealed in aluminum pans. The sample was first heated at 543 K, i.e. above the equilibrium melting temperature of an infinite crystal  $T_m^0$  (533 K for PA6). A dwell time of 8 min was used in order to erase the thermal history. The sample was then cooled down at  $-150$  K min<sup>-1</sup> to different isothermal temperature  $T_{iso,c}$  between 453 and 463 K (every 2 K). Crystallization control tests at  $-10$  K min<sup>-1</sup> were repeated before and after the campaign and confirmed the sample stability along the thermal cycles.

The heat flow curves of crystallization are presented in Fig. 2. The higher the applied temperature  $T_{iso,c}$ , the slower the kinetics and longer induction time, which is expected in this temperature range for PA6 [45] since the supercooling is lower. The crystallization is also characterized by unsymmetric peaks that reflect a kinetic slowdown at the end of the crystallization and suggests the existence of a secondary crystallization [46].

Fig. 3 shows the superposition of the crystallization curve obtained from the melt at  $T_{iso,c} = 453$  and 463 K with the second peak (corresponding to the crystallization) of the synthesis curve at the same temperature. The good agreement between curves indicates that when crystallization occurs separately from the polymerization, its kinetics correspond to the one obtained from the melt. This result suggests that the crystallization process is similar during synthesis and from the melt when polymerization and crystallization are almost decoupled.

## 3. Numerical methods

### 3.1. Synthesis kinetic formulation

By using a normalized kinetic formulation, the synthesis kinetics are expressed irrespective of the enthalpies associated to polymerization and crystallization. A weight factor of polymerization  $w_p$  [–] has been

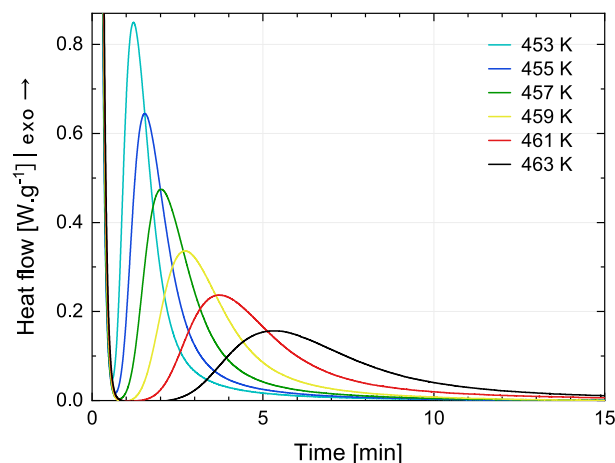


Fig. 2. Isothermal crystallization from the melt of a PA6 sample previously polymerized at  $T_{iso} = 423$  K.

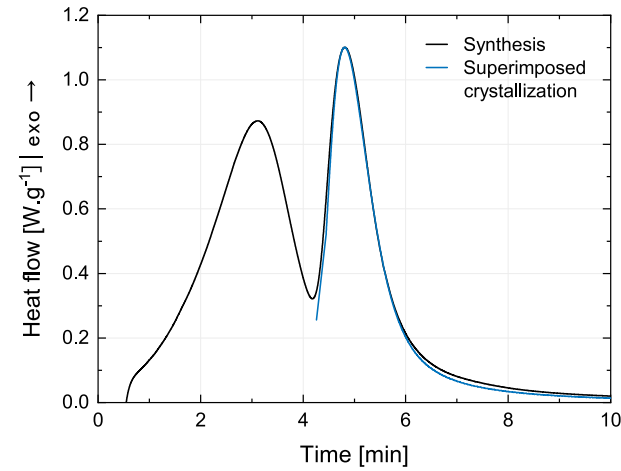
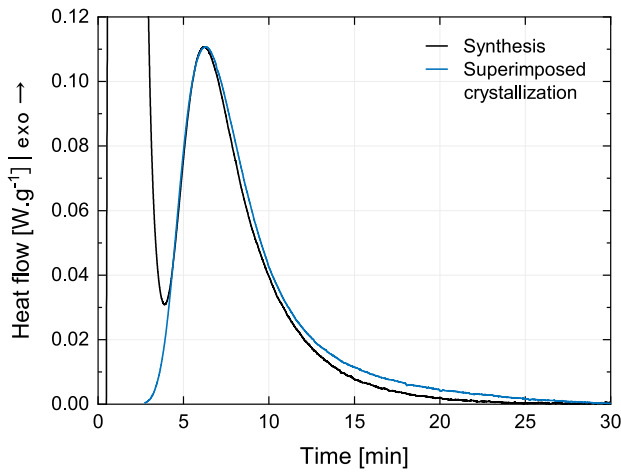
(a)  $T_{iso} = 453$  K(b)  $T_{iso} = 463$  K

Fig. 3. Superposition of isothermal crystallization curves obtained from the melt with the crystallization peak recorded during synthesis at the same temperature.

defined as the ratio of the final enthalpy of polymerization  $\Delta H_p^\infty$  to the total heat of reaction  $Q_{tot}$  according to equation (7). The weight factor of crystallization  $w_c$  [–] is defined in a similar manner, involving  $w_p + w_c = 1$ .

$$w_p(T) = \frac{\Delta H_p^\infty(T)}{Q_{tot}(T)} = \frac{\Delta H_p^\infty}{\Delta H_p^\infty + \Delta H_c^\infty(T)} \quad (7)$$

As shown in Table 1, the total heat of reaction  $Q_{tot}$  decreases with the increase in the synthesis temperature, while the mass fraction of polymerization  $X_p^\infty$  remains globally constant whatever the synthesis condition, with an average of  $\bar{X}_p^\infty = 94.2 \pm 1.4$  wt%. The weight factors  $w_p$  and  $w_c$  were therefore mainly dependent on the variation of crystallization enthalpy  $\Delta H_c$  with temperature. For sake of simplicity, a constant value was thus considered for the final enthalpy of polymerization  $\Delta H_p^\infty$ . It was calculated from the average mass fraction of polymerization  $\bar{X}_p^\infty$  and the theoretical total enthalpy of polymerization  $\Delta H_p^{100\%}$ .

As for crystallization, a second-order polynomial equation (eq. (8)) was used to model the temperature dependence of  $\Delta H_c^\infty(T)$  (Fig. 4). Beyond the roots of the polynomial curve, i.e. below 365.4 K and above 472.4 K, the crystallization was assumed impossible which was in good agreement with experimental observations reported in Ref. [10].

$$\Delta H_c^\infty(T) = -0.0354T^2 + 29.651T - 6107.5 \quad (8)$$

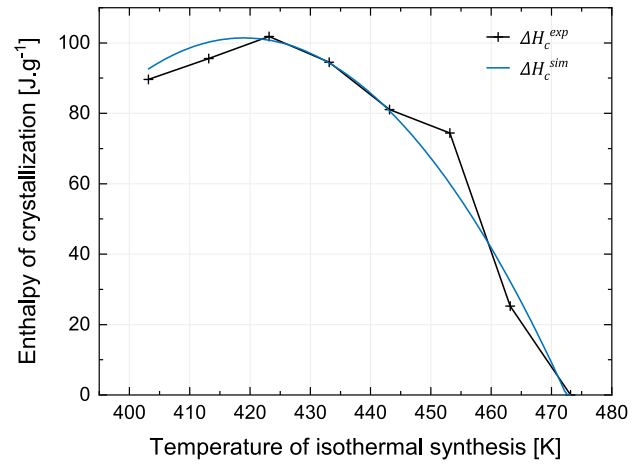


Fig. 4. Temperature dependence of the crystallization enthalpy  $\Delta H_c^\infty$  and second-order polynomial fit.

Using eqs. (7) and (8), the degree of global transformation  $\gamma$  (eq. (6)) can be used to define the coupling equation without using enthalpies of phenomena. The Malkin coupling model (eq. (5)) can be thus rearranged as equation (9).

$$\gamma(t) = w_p(T)\alpha(t) + (1 - w_p(T)) \underbrace{\int_0^t \alpha(\theta) \frac{d}{d\theta} \beta(\theta) d\theta}_{B(t)} \quad (9)$$

### 3.2. Model parameters identification procedure

The polymerization, crystallization and coupling models were identified sequentially on the experimental data of the degree of conversion  $\alpha$ , the degree of crystallinity  $\beta$  and the degree of global transformation  $\gamma$  respectively. A least squares method involving an interior-point optimization algorithm developed in Matlab® was used for determining model parameters. The identification was achieved on all datasets together, meaning that temperature dependent parameters and constant parameters could be distinguished.

The objective function was normalized by the number of data points on curves  $N_m$  (eq. (10)) and by the number of curves  $N_c$  (eq. (11)). The identification was run several times with different sets of initial parameters in order to avoid the convergence of the optimization algorithm into a local minimum set of parameters.

$$f_j(x) = \sqrt{\frac{1}{N_m} \sum_{i=1}^{N_m} \left( \frac{Y_{j,i}^{exp} - Y_{j,i}^{sim}(x)}{\max(Y_j^{exp})} \right)^2} \quad (10)$$

$$f_{tot}(x) = \frac{1}{N_c} \sum_{j=1}^{N_c} f_j(x) \quad (11)$$

## 4. Polymerization and crystallization models

### 4.1. Isothermal polymerization modeling

The polymerization kinetics  $\dot{\alpha}$  were described by the differential equation (12) proposed by Camargo et al. [29] based on Malkin's work [22,24,28]. This model presents an Arrhenius temperature dependence in which  $A_0$  [s<sup>-1</sup>] is a constant representative of the number of collisions between molecules,  $B_0$  [–] is an autocatalytic factor,  $n_p$  [–] corresponds to the reaction order,  $E_a$  [J mol<sup>-1</sup>] is the activation energy of the polymerization and  $R$  [J K<sup>-1</sup> mol<sup>-1</sup>] is the universal gas constant.

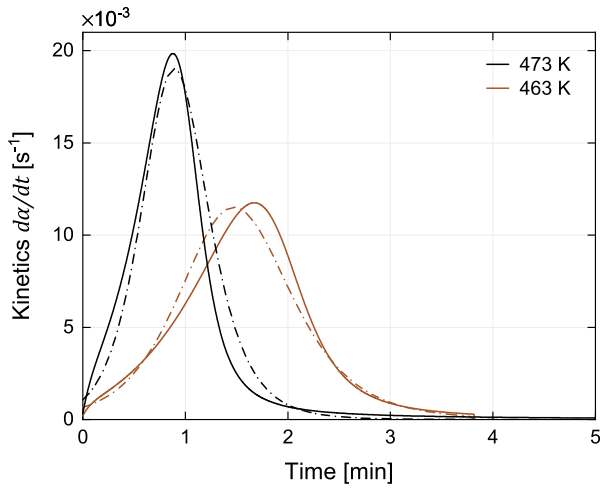


Fig. 5. Simulation of decoupled isothermal polymerization with Malkin-Camargo model; (—) *exp* and (---) *sim*.

$$\frac{d\alpha}{dt} = A_0(1 - \alpha)^{n_p}(1 + B_0\alpha)\exp\left(-\frac{E_a}{RT}\right) \quad (12)$$

Between 463 and 473 K, the polymerization peak is completely separated from the crystallization, which allowed the assessment of the four parameters of the Malkin-Camargo model by optimization. Fig. 5 compares the experimental polymerization kinetics  $\dot{\alpha}$  with the model prediction. The good agreement between results demonstrates the relevance of the model. Final parameters of the model were optimized with the coupling model and the full temperature range of isothermal synthesis.

#### 4.2. Isothermal crystallization modeling

As previously mentioned, crystallization during synthesis is similar to crystallization from the melt (Fig. 3) when it is decoupled from the polymerization ( $T_{iso} = 453$  and 463 K). It was thus decided to identify the crystallization model from results recorded on the synthesized PA6 sample and presented in Fig. 2. This strategy to model crystallization from bulk crystallization was postulated by Malkin et al. [23,25,37–39]. It implies that the interaction with the polymerization progress is only considered through the coupling equation.

Among available models describing the crystallization from the melt of thermoplastic polymer, the Nakamura model [47,48] was selected as it enables modeling isothermal and non-isothermal crystallization with a unique simple equation. The relative degree of crystallinity  $\beta$  was expressed with equation (13), in which  $K_N$  [ $s^{-1}$ ] is the Nakamura global kinetic constant and  $n$  [–] the Avrami exponent distinctive of the type of nucleation (instantaneous or sporadic) and geometry of crystal growth.

$$\beta(t) = 1 - \exp\left(-\left(\int_0^t K_N(T(\theta)) d\theta\right)^n\right) \quad (13)$$

The temperature dependent kinetic constant  $K_N(T)$  was modeled using the Hoffman-Lauritzen equation (eq. (14)) [49]. In equation (14),  $U^*$  refers to the activation energy of macromolecular motion in the molten state, that was set to  $6300 \text{ J mol}^{-1}$ ,  $K_g$  is a constant related to crystallization growth, the temperature  $T^\infty$  corresponds to the difference  $T_g - 30 \text{ K}$ ,  $T_m^0$  refers to the equilibrium melting temperature of PA6 crystals and  $f$  defines a corrective factor introduced by Hoffman for high supercooling conditions. This factor is given by the relation  $f = \frac{2T}{(T_m^0 + T)}$ . The parameters  $n$ ,  $K_0$  and  $K_g$  were determined by optimization while  $T_\infty$  and  $T_m^0$  were set to 293 K and 533 K respectively [50].

$$K_N(T) = K_0 \exp\left(-\frac{U^*}{R(T - T_\infty)}\right) \exp\left(-\frac{K_g}{T(T_m^0 - T)f}\right) \quad (14)$$

The main advantage of this model is that it considers the temperature dependence of macromolecular diffusion and nucleation in a temperature range lasting from the glass transition temperature up to the equilibrium melting temperature of PA6 crystal  $T_m^0$ . It allows representing the maximum crystallization kinetics around 413 K and the reduction of crystallization kinetics close to  $T_g$  and  $T_m^0$ , that have been observed for PA6 by McGill on spherulite growth rate [45] or by fast scan DSC measurements more recently [51,52].

Besides the crystallization kinetic equation, an induction time  $t_{c,0}(T)$  was introduced in the model in order to consider the time required for the nucleus to form before crystal growth can start. This induction time was modeled with an Arrhenius equation related to the equilibrium melting temperature  $T_m^0$  (eq. (15)). The induction time introduced two parameters to be identified by optimization: a pre-exponential factor  $A_i$  and an activation energy  $E_i$ .

$$t_{c,0}(T) = A_i \exp\left(\frac{E_i}{R(T_m^0 - T)}\right) \quad (15)$$

Fig. 6 compares the measured crystallization kinetics  $\dot{\beta}$  and the model predictions (eqs. (13) and (14)); here the time is normalized with the induction time, i.e.  $t - t_{c,0}$ . The latter observed experimentally (Fig. 2) is compared with the Arrhenius model (eq. (15)) in Fig. 7.

Results in Fig. 6 are in good agreement except by the end of crystallization where a possible secondary crystallization can occur. In order to take into account this phenomenon, a coupling equation between two crystallization models could be used, like the couplings proposed by Hillier [42], Velisaris and Seferis [53] or Cebe [54]. However it was decided to limit the complexity of the crystallization model to a single Nakamura model. It is indeed aimed at modeling PA6 crystallization during synthesis between 403 and 473 K but it was identified on experimental curves recorded only between 453 and 463 K. The extrapolation of the crystallization model was therefore considered critical with regards to the secondary crystallization process and a reduced number of parameters was preferred.

Table 2 presents the crystallization parameters obtained by the global optimization. It appears that  $n$  is relatively small and is not consistent with the spherulitic geometry usually observed for PA6 crystallized from the melt. This result could be a consequence of using a unique Nakamura model to represent the entire transformation without considering the secondary crystallization. Parameters obtained are thus an average of the ones attributed to each mechanism. The crystallization parameters identified from the melt will be fixed for the coupling modeling, being therefore excluded to the global optimization.

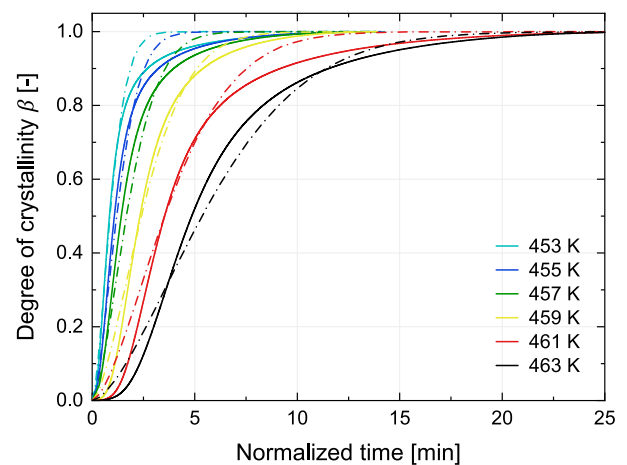


Fig. 6. Simulation of the relative degree of crystallinity during the bulk crystallization of a synthesized PA6 sample; (—)  $\dot{\beta}_{exp}$  and (---)  $\dot{\beta}_{sim}$ .



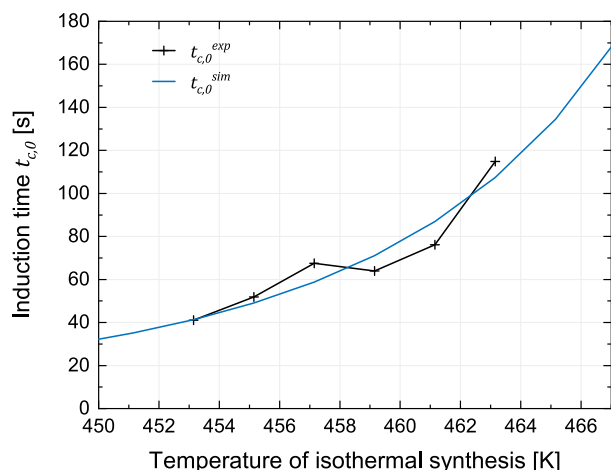


Fig. 7. Simulation of the induction time  $t_{c,0}$  appearing prior crystallization from the melt of a synthesized PA6 sample.

Table 2

Parameters of Nakamura-Hoffman-Lauritzen model identified by optimization on curves of crystallization from the melt.

Parameter	Value	Unit
$K_0$	$7.59 \times 10^8$	$[s^{-n}]$
$K_g$	$6.63 \times 10^5$	$[K^2]$
$N$	1.59	$[-]$
$A_t$	$5.17 \times 10^{-2}$	$[s^{-1}]$
$E_t$	4.45	$[kJ \text{ mol}^{-1}]$

Fig. 8 shows the crystallization curves simulated with Nakamura-Hoffman-Lauritzen model and the induction time over the temperature range used for PA6 synthesis from  $\epsilon$ -caprolactam, i.e. from 403 to 473 K. At low temperature, where  $K_N$  is maximal, crystallization only lasts 10 s. Conversely, 5 h are required to complete crystallization at 473 K.

## 5. Coupling modeling

### 5.1. Malkin coupling

In order to take into account the coupling between polymerization and crystallization, Malkin et al. [23,25] proposed that the term due to crystallization depends on the degree of conversion  $\alpha$  achieved at time  $t$  as shown in equation (5) and rearranged as equation (9) using equations (1)–(7). This coupling has been used in the literature to model the temperature rising during adiabatic syntheses [13,23,25,55].

The introduction of the induction time of crystallization  $t_{c,0}$  gives equation (16), which distinguishes two cases depending on the sign of  $\theta - t_{c,0}(T)$  described with the Heaviside step function  $H$ .

$$\gamma(t) = w_p(T)\alpha(t) + (1 - w_p(T)) \times \underbrace{\int_0^t H(\theta - t_{c,0}(T))\alpha(\theta) \frac{d}{d\theta} \beta(\theta - t_{c,0}(T)) d\theta}_{B(t)} \quad (16)$$

This coupling assumes that both polymerization and crystallization start at the beginning of the reaction and occur at the same time. It means that at each new increment of polymerization, the formed phase is involved in the global crystallization in progress. Moreover, it does not consider the possible influence of the crystallization on the polymerization at low synthesis temperature, even if this possibility has been mentioned in literature [5,7,10,12,13].

Fig. 9 presents results at  $T_{iso} = 413$  and 443 K obtained with Malkin coupling (eq. (16)), the Malkin-Camargo polymerization model (eq.

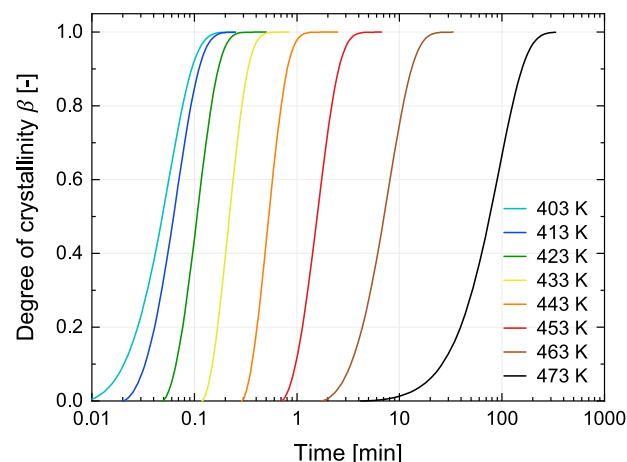


Fig. 8. Simulation of the degree of crystallinity  $\beta$  through the Nakamura-Hoffman-Lauritzen model including the induction time  $t_{c,0}$  over the temperature range of PA6 isothermal synthesis.

(12)) and the Nakamura-Hoffman-Lauritzen crystallization model (eqs. (13)–(15)) compared to experimental data from DSC. Fig. A in Supplementary data gathers the synthesis curves simulated from  $T_{iso} = 403$ –473 K. It appears that this coupling equation completely inhibits crystallization.

These results are a direct consequence of the form of the term  $B$  in the Malkin coupling (eq. (16)), which could reach 1 only if phenomena are perfectly decoupled, i.e. if the polymerization is completed ( $\alpha = 1$ ) prior to crystallization. However, the crystallization model extrapolation, especially at low temperature (403–423 K), implies very high kinetics (Fig. 8) within a time scale of tens of seconds while the polymerization takes one to 2 h. The product of the two components in term  $B$  is thus almost zero and leads to a reaction only described by the polymerization kinetics.

This incoherence is inherent of the hypothesis of a global crystallization starting at the beginning of the synthesis. At low temperature, it means both that the crystallization starts even though chains are not yet polymerized, and that chains formed after the end of the global crystallization cannot crystallize despite the thermal conditions being favorable for a crystalline organization.

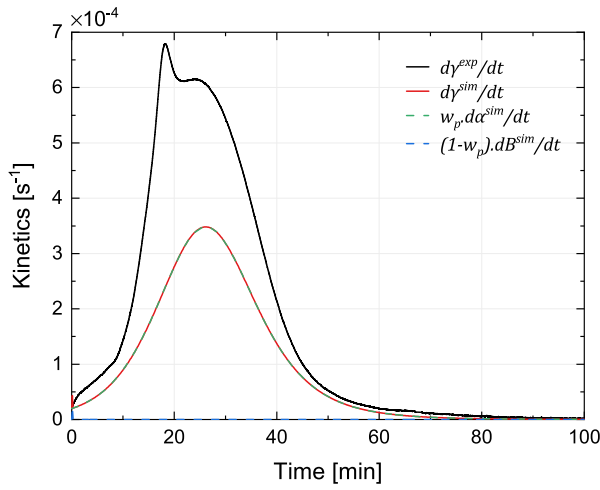
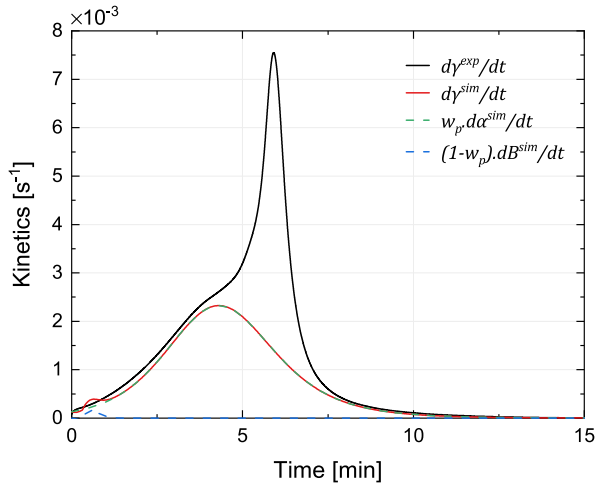
### 5.2. Hillier coupling

In order to counterbalance the lack of physical meaning involved in the Malkin coupling, the Hillier equation [42] has been adapted to the case of the PA6 polymerization and crystallization coupling (eq. (17)). The difference with the Malkin coupling (eq. (9)) is in the time dependence of the local decoupled crystallization term  $\beta$ . Indeed the term  $B$ , which represents the coupled crystallization, corresponds here to the degree of crystallinity at time  $t$  of an element that was polymerized at time  $\theta$ . In other words, each new polymerized part (new increment of  $\alpha$ ) starts its crystallization with its own initiation time and its own kinetics.

Hillier coupling thus represents the influence of polymerization on crystallization in terms of the availability of chain segments, which corresponds to the experimental observations. Nevertheless, as with the Malkin coupling, this adaptation of Hillier coupling assumes that crystallization does not influence polymerization, although this possibility has been mentioned previously [1].

$$\gamma(t) = w_p(T)\alpha(t) - (1 - w_p(T)) \underbrace{\int_0^t \alpha(\theta) \frac{d}{d\theta} \beta(t - \theta) d\theta}_{-B(t)} \quad (17)$$

By introducing the crystallization induction time  $t_{c,0}$  (eq. (15)) into equation (17), the coupling is described according to equation (18),

(a)  $T_{iso} = 413$  K(b)  $T_{iso} = 443$  K

**Fig. 9.** Simulation of PA6 synthesis kinetics  $\dot{\gamma}$ , polymerization kinetics  $\dot{\alpha}$  and crystallization kinetics  $\dot{B}$  with Malkin coupling (eq. (16)) versus DSC data.

where  $H$  is the Heaviside step function.

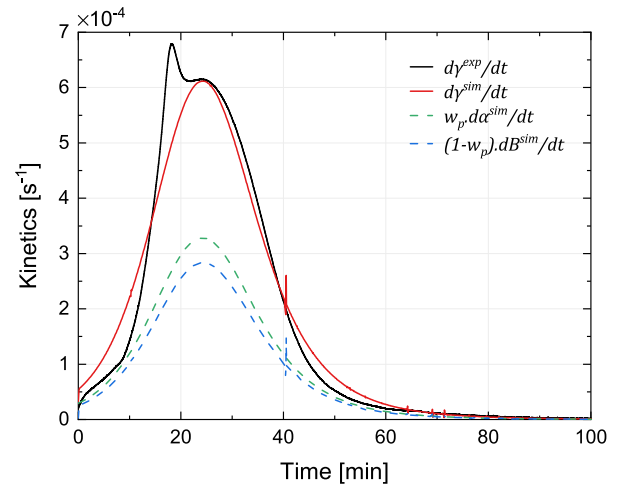
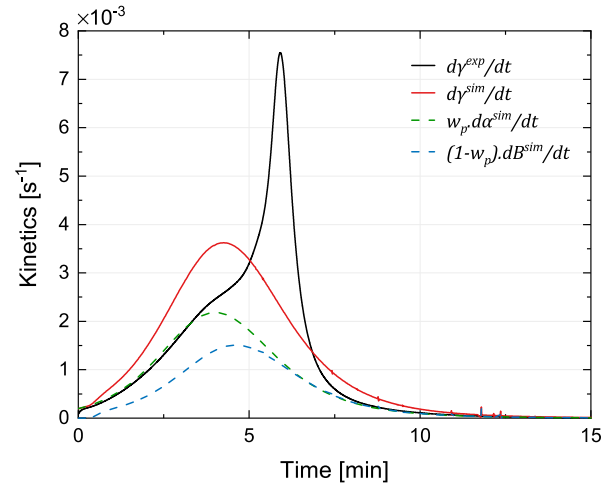
$$\gamma(t) = w_p(T)\alpha(t) - (1 - w_p(T)) \times \int_0^t H(t - \theta - t_{c,0}(T))\alpha(\theta) \frac{d}{d\theta} \beta(t - \theta - t_{c,0}(T)) d\theta \quad (18)$$

with:

$$\begin{aligned} \frac{d}{d\theta} \beta(t - \theta - t_{c,0}(T)) = & \\ & - \exp(-(\int_0^{t-\theta-t_{c,0}(T)} K_N(T) d\tau)^n) \\ & nK_N(T)(\int_0^{t-\theta-t_{c,0}(T)} K_N(T) d\tau)^{n-1} \end{aligned}$$

The identification of the four parameters of the Malkin-Camargo polymerization model (eq. (12)) was performed on the  $\gamma$  sigmoid obtained for the isothermal syntheses between 403 and 473 K (every 10 K).

Fig. 10 details the kinetic curves simulated at 413 and 443 K compared to experimental data from DSC and Fig. B in Supplementary data gathers the synthesis curves simulated from  $T_{iso} = 403$ –473 K. Unlike the Malkin coupling, the crystallization is predicted for all temperatures. At low temperature, the crystallization is limited by the polymerization and then adopts its kinetics, since each new increment crystallizes almost instantaneously. This is consistent with the interpretation of the kinetic results obtained in Ref. [10]. At 463 K, the coupling slightly shifts the crystallization compared to the Malkin

(a)  $T_{iso} = 413$  K(b)  $T_{iso} = 443$  K

**Fig. 10.** Simulation of PA6 synthesis kinetics  $\dot{\gamma}$ , polymerization kinetics  $\dot{\alpha}$  and crystallization kinetics  $\dot{B}$  with Hillier coupling (eq. (18)) versus DSC data.

coupling, which improves the prediction (see Fig. B).

However, since the crystallization starts at the beginning of the polymerization, the model does not reproduce the crystallization peaks in the early stages of the polymerization between 403 and 413 K and the shoulders observed between 423 and 443 K. As previously mentioned, these peaks are due to the germination that cannot start in the first moments of the polymerization. Thus at 413 K (Fig. 10a), the germination seems to start from about 10 min and at 443 K (Fig. 10b) after 4 min. The induction time of the crystallization  $t_{c,0}$  only translates the influence of the temperature on the crystallization initiation and does not consider the effect of molar masses or the concentrations reached.

If the use of the Hillier coupling with the Malkin-Camargo and Nakamura-Hoffman-Lauritzen crystallization models improves the simulation of PA6 synthesis by correcting the absence of crystallization at low temperature predicted with the Malkin coupling, all the physical phenomena are not taken into account. The introduction of a corrective factor in the crystallization term  $B$  was therefore proposed in order to improve the prediction of synthesis kinetics.

### 5.3. Corrective factor

An empirical corrective factor was added to the coupling equation to correct the particular crystallization kinetics observed during early

stages of polymerization at the low temperature, i.e. between 403 and 443 K. It was inspired by the diffusion factor introduced in thermosetting curing models to take into account the drastic decrease of the crosslinking kinetics due to vitrification. The corrective factor  $f_d$  in equation (20) depends on the degree of conversion  $\alpha$  and the temperature  $T$ .  $f_d$  displays a sigmoid shape defined between 0 and 1 and parametrized by  $C$  and  $D$  [–], which govern the half-height slope and the shift of  $f_d$  sigmoid on  $\alpha$  axis respectively.

$$f_d(\alpha, T) = 1 - \frac{1}{1 + \exp(C(T)(\alpha - 1) + D(T))} \quad (19)$$

adding the corrective factor  $f_d$  into the coupling equation (18) gives equation (21).

$$\gamma(t) = w_p(T)\alpha(t) - (1 - w_p(T)) \times \int_0^t H(t - \theta - t_{c,0}(T))f_d(\alpha(\theta), T)\alpha(\theta)\frac{d}{d\theta}\beta(t - \theta - t_{c,0}(T))d\theta \quad (20)$$

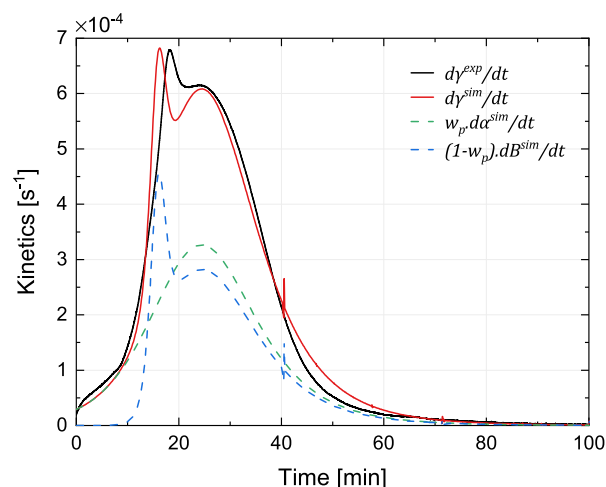
An overall optimization was performed on sigmoidal  $\gamma$  curves of isothermal syntheses in order to refine the four parameters of the Malkin-Camargo polymerization model (eq. (12)) and to identify parameters  $C$  and  $D$  for each  $T_{iso}$  since their temperature dependence is not known *a priori*. For their identification, constraints were imposed on these parameters:  $D$  was set higher than 6.9 in order to get  $f_d(0.999, T) = 1$  and  $C - D > 6.9$  to get  $f_d(0.001, T) = 0$ .

Fig. 11 details the kinetic curves simulated at  $T_{iso} = 413$  and 443 K compared to experimental data from DSC. Results of all synthesis temperatures are presented in Figs. C to F in Supplementary data. The results clearly show the contribution of the corrective factor  $f_d$ , as the model reproduces the particular crystallization kinetic behavior observed at the beginning of polymerization by delaying its initiation.

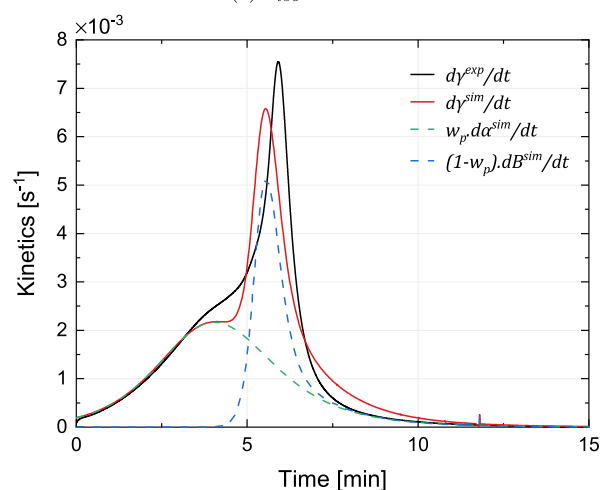
Fig. 12 presents the evolution of the corrective factor  $f_d$  as a function of the degree of conversion  $\alpha$  for each temperature. The higher the synthesis temperature, the higher the degree of conversion  $\alpha$  for which the sigmoid  $f_d$  proceeded. This is consistent with the fact that the higher the temperature, the higher the critical nucleus size to reach and therefore the higher the molar mass or the concentration. At higher temperature ( $T_{iso}$  between 453 and 463 K)  $f_d$  has little effect since the induction time of crystallization  $t_{c,0}$  is enough to take into account the late crystallization observed. It is consistent with the experimental observations presented previously (Fig. 1): the crystallization is decoupled from the polymerization and its kinetics is similar to that taking place from the molten state. At 473 K crystallization does not occur, meaning that  $f_d$  has no effect at this temperature.

Fig. 13 shows the evolution of the parameters  $C$  and  $D$  as a function of the synthesis temperature. No proper model was found to correctly represent their temperature dependence due to the high sensitivity to parameters  $C$  and  $D$ . The values necessary for the simulation of the synthesis at other isothermal temperatures or under non-isothermal conditions were thus interpolated from the parameters  $C$  and  $D$  identified at the different  $T_{iso}$ .

Table 3 summarizes the polymerization parameters obtained by a global optimization with the Hillier coupling and the corrective factor  $f_d$ . The activation energy of the reaction  $E_a$  reaches more than 90 kJ mol<sup>−1</sup>, whereas the values reported in the literature with the same catalyst (MgBrCL) are between 53 and 84 kJ mol<sup>−1</sup> [12,55,56]. However, it should be noted that the results of Davé et al. [12] and Teuwen [55] were obtained by modeling the temperature rise of the medium in an adiabatic reactor, which limits the measurement sensitivity for an accurate characterization of the temperature dependence of phenomena contrary to the DSC characterization used in this study. Moreover, results of Merna et al. [56] correspond to copolymerization with the  $\epsilon$ -caprolactone monomer (forming polycaprolactone), which may explain the different activation energies  $E_a$  obtained. In the literature, most of the modeling studies have focused on the sodium caprolactamate (NaCL) catalyst, which has a reaction activation energy  $E_a$  comprised between 62.8 and 104.3 kJ mol<sup>−1</sup>



(a)  $T_{iso} = 413$  K



(b)  $T_{iso} = 443$  K

Fig. 11. Simulation of PA6 synthesis kinetics  $\dot{\gamma}$ , polymerization kinetics  $\dot{\alpha}$  and crystallization kinetics  $\dot{B}$  with Hillier coupling including the corrective factor  $f_d$  (eq. (21)) versus DSC data.

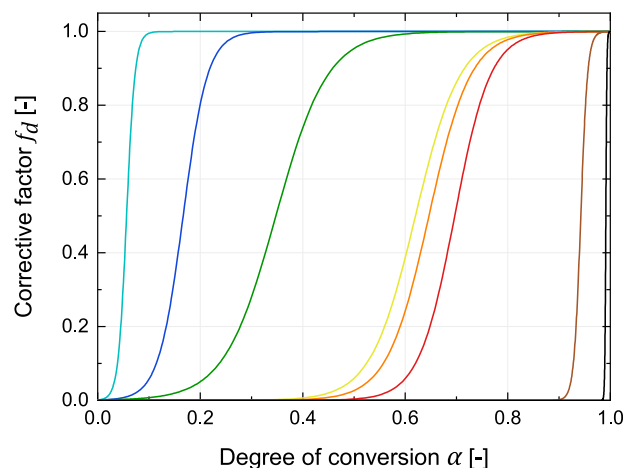


Fig. 12. Evolution of the corrective factor  $f_d$  with the degree of conversion  $\alpha$  for the different synthesis temperatures  $T_{iso}$

[13,22,24,25,29,31,32,57] for adiabatic synthesis.

The reaction order  $n_p$  identified is in good agreement with literature for the MgBrCL catalyst [12,55], which reports values between 0.93



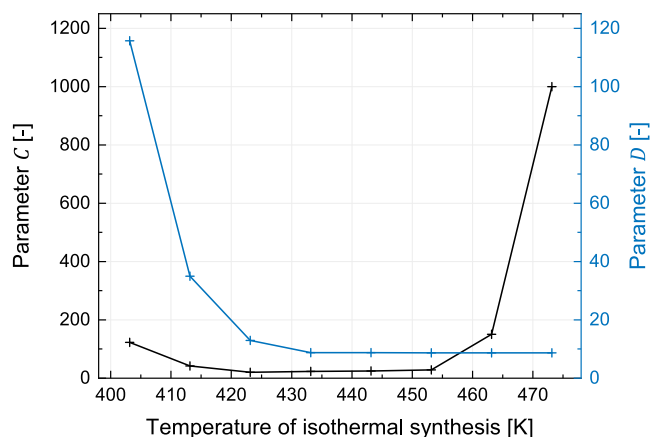


Fig. 13. Parameters  $C$  and  $D$  of the corrective factor  $f_d$  versus synthesis temperature  $T_{iso}$ .

Table 3

Parameters of Malkin-Camargo polymerization model identified by optimization on synthesis curves with Hillier coupling, Nakamura-Hoffman-Lauritzen- $t_{c,0}$  crystallization model and corrective factor  $f_d$ .

Parameter	Value	Unit
$A_0$	$1.86 \times 10^7$	$[s^{-1}]$
$E_a$	91.2	$[kJ\ mol^{-1}]$
$B_0$	47.4	$[-]$
$n_p$	1.14	$[-]$

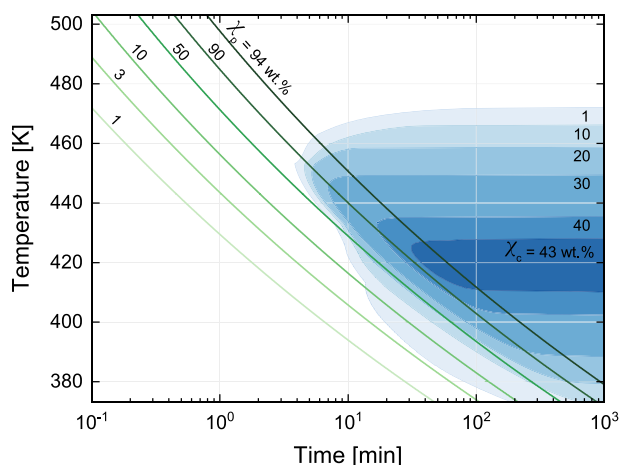


Fig. 14. Simulated isothermal TTT diagram of PA6 synthesis.

and 1.2. The autocatalytic factor  $B_0$  is greater than the range of 7–21 reported by literature [12,55]. Finally, the parameter  $A_0$  is hardly comparable because its value depends directly on the identified activation energy  $E_a$  (Arrhenius law).

This empirical corrective factor reveals current limits of the coupling equation proposed in this study. The influence of the polymerization on crystallization at the early stages of synthesis could be achieved by introducing polymerization-dependent parameters into the crystallization model, instead of adding a corrective factor dependent on the degree of conversion  $\alpha$ . The crystallization kinetic parameters would be either temperature dependent and functions of the molecular weight, as already evoked in the literature [58,59], or the chain concentration within the mixture. However, this would increase the level of complexity of the identification of parameters as it can no longer be separately identified on crystallization from the melt of a synthesized PA6.

In addition, the influence of crystallization on the polymerization should be considered in a further improvement of the synthesis kinetic model as it affects the degree of conversion  $X_p^\infty$  for  $T_{iso} < 443\ K$  [10].

#### 5.4. Time-Temperature-Transformation diagram

Isothermal TTT diagram of the PA6 synthesis was developed due to the new model proposed in this study and is shown on Fig. 14. This diagram represents iso-polymerization curves ( $X_p$  from 1 to 94 wt% in green) and iso-crystallinity curves ( $X_c$  from 1 to 43 wt% in blue). This diagram must be horizontally read at a constant temperature. Readers should keep in mind that the studied experimental range is between 403 and 473 K, thus simulations outside of these boundaries have not been characterized.

The strong coupling between polymerization and crystallization appears clearly on Fig. 14 for low synthesis temperature (383–433 K), since the crystallization is restrained by the polymerization progress. At higher temperature, phenomena progressively separate due to the polymerization acceleration and crystallization deceleration, until a limit temperature of 468 K, above which the newly formed chains do not crystallize.

## 6. Conclusion

The Hillier's formalism demonstrated its ability in predicting the overall synthesis of polyamide 6 from its monomer  $\epsilon$ -caprolactam. It accurately describes the influence of polymerization on the crystallization kinetics when synthesis is achieved at high temperature, i.e. when the coupling level of both phenomena is limited. This coupling equation resolves the lack of physical meaning of previous models from the literature as the level of coupling does not affect the final crystallization enthalpy.

Although the sole coupling fails in predicting the synthesis kinetics when crystallization is faster than polymerization at low temperature, it allows consideration that a PA6 molecule crystallizes as in bulk case with its own kinetics from the moment it is polymerized, but it does not consider the case of short molecules crystallizing in a dilute medium of reactive mixture.

This can be solved by introducing a corrective factor into the coupling without modifying the bulk crystallization model. This empirical factor, which depends on the degree of conversion  $\alpha$  and temperature, provides a convenient and simple solution for that purpose. A better understanding of the crystallization of low molecular weight PA6 in the reactive mixture is however required to obtain a predictive modeling of PA6 synthesis that is suitable for non-isothermal modeling as well. An alternative to that corrective factor could be a crystallization model involving parameters that directly depend on the degree of conversion  $\alpha$ .

## Appendix A. Supplementary data

Supplementary data to this article can be found online at <https://doi.org/10.1016/j.polymer.2019.121681>.

## References

- [1] K. van Rijswijk, H.E.N. Bersee, Reactive processing of textile fiber-reinforced thermoplastic composites - an overview, *Compos. Appl. Sci. Manuf.* 38 (2007) 666–681.
- [2] K. Khodabakhshi, M. Gilbert, P. Dickens, Monitoring of small-scale anionic polymerization of caprolactam; a method to be used in an additive manufacturing process, *Polym. Adv. Technol.* 24 (2013) 503–510.
- [3] K. Khodabakhshi, M. Gilbert, S. Fathi, P. Dickens, Anionic polymerisation of caprolactam at the small-scale via DSC investigations, *J. Therm. Anal. Calorim.* 115 (1) (2014) 383–391.
- [4] O. Wichterle, J. Sebenda, J. Kralicek, The anionic polymerization of caprolactam, *Adv. Polym. Sci.* 2/4 (1961) 578–595.
- [5] T. Komoto, M. Iguchi, H. Kanetsuna, T. Kawai, Formation of spherulites during

- polymerization of lactams, *Makromol. Chem.* 135 (1) (1970) 145–164.
- [6] O. Wichterle, J. Sebenda, J. Tomka, Adiabatic crystallization of amorphous polycaprolactame, *J. Polym. Sci. B Polym. Phys.* 57 (1962) 785–791.
  - [7] B. Wunderlich, *Macromolecular Physics - Crystal Nucleation Growth Annealing* vol. 2, Academic Press, 1976.
  - [8] V.V. Korshak, T.M. Frunze, S.P. Davtyan, V.V. Kurashev, T.V. Volkova, V.A. Kotelnikov, R.B. Shleifman, Kinetics of activated anionic polymerization of  $\epsilon$ -caprolactam under non-isothermal conditions, *Polym. Sci. U. S. S. R.* 21 (9) (1979) 2161–2169.
  - [9] S.P. Davtyan, P.V. Zhirkov, S.A. Vol'fon, Problems of non-isothermal character in polymerisation processes, *Russ. Chem. Rev.* 53 (2) (1984) 150.
  - [10] Céline Vicard, Olivier De Almeida, Cantarel Arthur, Gérard Bernhart, Experimental study of polymerization and crystallization kinetics of polyamide 6 obtained by anionic ring opening polymerization of  $\epsilon$ -caprolactam, *Polymer* 132 (Supplement C) (2017) 88–97.
  - [11] K. van Rijswijk, *Thermoplastic Composite Wind Turbine Blades - Vacuum Infusion Technology for Anionic Polyamide-6 Composites*, Thèse, Technische Universiteit Delft, 2007.
  - [12] R.S. Davé, K. Udipi, R.L. Kruse, L.R. Stebbins, Polyamides from lactams via anionic ring-opening polymerization: 2. Kinetics, *Polymer* 38 (4) (1997) 939–947.
  - [13] K.H. Lee, S.C. Kim, Reaction-induced crystallization kinetics during the anionic polymerization of  $\epsilon$ -caprolactam, *Polym. Eng. Sci.* 28 (1) (1988) 13–19.
  - [14] A. Luisier, P.E. Bourban, J.-A.E. Månson, Time-Temperature-Transformation diagram for reactive processing of polyamide 12, *J. Appl. Polym. Sci.* 81 (4) (2001) 963–972.
  - [15] E. Sittler, J. Sebenda, Alkaline polymerization of 6-caprolactam. XXXII. The kinetics of polymerization activated by N,N,N',N'-tetraacetylhexamethylenediamine, *Collect. Czechoslov. Chem. Commun.* 33 (1968) 270–277.
  - [16] R.Z. Greenley, J.C. Stauffer, J.E. Kurz, The kinetic equation for the initiated anionic polymerization of  $\epsilon$ -caprolactam, *Macromolecules* 2 (6) (1969) 561–567.
  - [17] H.K. Reimschuessel, Ring-Opening Polymerization, Chapter Chapter 7. Kinetics of Hydrolytic Polymerization, Marcel Dekker, 1969, pp. 303–326.
  - [18] A. Rigo, G. Fabbri, G. Talamini, Kinetic study of anionic polymerization of 6-caprolactam by differential calorimetry, *J. Polym. Sci., Polym. Lett. Ed.* 13 (8) (1975) 469–477.
  - [19] D.J. Lin, J.M. Ottino, E.L. Thomas, A kinetic study of the activated anionic polymerization of  $\epsilon$ -caprolactam, *Polym. Eng. Sci.* 25 (18) (Dec 1985) 1155–1163.
  - [20] R.A. Cimini, D.C. Sundberg, A mechanistic kinetic model for the initiated anionic polymerization of  $\epsilon$ -caprolactam, *Polym. Eng. Sci.* 26 (8) (1986) 560–568.
  - [21] P. Wittmer, H. Gerrens, Über die anionische schnellpolymerisation von caprolactam, *Makromol. Chem.* 89 (27) (1965).
  - [22] A. Ya Malkin, V.G. Frolov, A.N. Ivanova, Z.S. Andrianova, The nonisothermal anionic polymerization of caprolactam, *Polym. Sci. U. S. S. R.* 21 (3) (1979) 691–700.
  - [23] S.A. Bolgov, V.P. Beghishev, A. Ya Malkin, V.G. Frolov, Role of the functionality of activators during isothermal crystallization accompanying the activated anionic polymerization of  $\epsilon$ -caprolactam, *Polym. Sci. U. S. S. R.* 23 (6) (1981) 1485–1492.
  - [24] A. Ya Malkin, S.L. Ivanova, V.G. Frolov, A.N. Ivanova, Z.S. Andrianova, Kinetics of anionic polymerization of lactams. (Solution of non-isothermal kinetic problems by the inverse method), *Polymer* 23 (12) (1982) 1791–1800.
  - [25] A. Ya Malkin, V.P. Beghishev, S.A. Bolgov, The exothermal effects of superimposed processes of activated anionic polymerization of  $\epsilon$ -caprolactam and crystallization of the polymer formed, *Polymer* 23 (3) (1982) 385–390.
  - [26] M.R. Kamal, S. Sourour, Kinetics and thermal characterization of thermoset cure, *Polym. Eng. Sci.* 13 (1) (1973) 59–64.
  - [27] S. Sourour, M.R. Kamal, Differential scanning calorimetry of epoxy cure: isothermal cure kinetics, *Thermochim. Acta* 14 (1–2) (1976) 41–59.
  - [28] A. Ya, Malkin. Rheology in polymerization processes, *Polym. Eng. Sci.* 20 (15) (1980) 1035–1044.
  - [29] R.E. Camargo, V.M. Gonzalez, C.W. Macosko, M. Tirrell, Bulk polymerization kinetics by the adiabatic reactor method, *Rubber Chem. Technol.* 56 (4) (1983) 774–783.
  - [30] J.-L. Yeh, J.-F. Kuo, C.-Y. Chen, Adiabatic anionic polymerization of caprolactam in the presence of N-acylated caprolactam macroactivator: kinetic study, *J. Appl. Polym. Sci.* 50 (10) (1993) 1671–1681.
  - [31] K.J. Kim, Y.Y. Kim, B.S. Yoon, K.J. Yoon, Mechanism and kinetics of adiabatic anionic polymerization of  $\epsilon$ -caprolactam in the presence of various activators, *J. Appl. Polym. Sci.* 57 (11) (1995) 1347–1358.
  - [32] K.J. Kim, D.S. Hong, A.R. Tripathy, Kinetics of adiabatic anionic copolymerization of  $\epsilon$ -caprolactam in the presence of various activators, *J. Appl. Polym. Sci.* 66 (6) (1997) 1195–1207.
  - [33] J.J.E. Teuwen, A.A. van Geenen, H.E.N. Bersee, Novel reaction kinetic model for anionic polyamide-6, *Macromol. Mater. Eng.* 298 (2) (2013) 163–173.
  - [34] S. Russo, S. Maniscalco, P. Moretti, L. Ricco, Fast-activated anionic polymerization of  $\epsilon$ -caprolactam in the bulk under quasi-adiabatic conditions: comparison of different kinetic models, *J. Polym. Sci. A Polym. Chem.* 51 (20) (2013) 4474–4480.
  - [35] J. Nagy, L. Reith, M. Fischlschweiger, G. Steinbichler, Modeling the influence of flow phenomena on the polymerization of  $\epsilon$ -caprolactam, *Chem. Eng. Sci.* 111 (0) (2014) 85–93.
  - [36] A. Ya Malkin, S.G. Kulochikhin, V.G. Frolov, M.I. Demina, Rheokinetics of anionic polymerization of caprolactam, *Polym. Sci. U. S. S. R.* 23 (6) (1981) 1471–1479.
  - [37] A. Ya Malkin, V.P. Beghishev, I.A. Keapin, Macrokinetics of polymer crystallization, *Polymer* 24 (1) (1983) 81–84.
  - [38] A. Ya Malkin, V.P. Beghishev, I.A. Keapin, S.A. Bolgov, General treatment of polymer crystallization kinetics - Part 1. A new macrokinetic equation and its experimental verification, *Polym. Eng. Sci.* 24 (18) (1984) 1396–1401.
  - [39] A. Ya Malkin, V.P. Beghishev, I.A. Keapin, Z.S. Andrianova, General treatment of polymer crystallization kinetics - Part 2. The kinetics of nonisothermal crystallization, *Polym. Eng. Sci.* 24 (18) (1984) 1402–1408.
  - [40] K. Taki, N. Shoji, M. Kobayashi, H. Ito, A kinetic model of viscosity development for in situ ring-opening anionic polymerization of  $\epsilon$ -caprolactam, *Microsyst. Technol.* 23 (5) (2017) 1161–1169.
  - [41] J.J.E. Teuwen, *Large Thermoplastic Composite Wind Turbine Blades - Process Optimization for Vacuum Infusion of Large Blades*, Technical Report, We@Sea, 2009.
  - [42] I.H. Hillier, Modified Avrami equation for the bulk crystallization kinetics of spherulitic polymers, *J. Polym. Sci. - Part A Gen. Pap.* 3 (9) (1965) 3067–3078.
  - [43] J.D. Hoffman, Theoretical aspects of polymer crystallization with chain folds: bulk polymers, *Polym. Eng. Sci.* 4 (4) (1964) 315–362.
  - [44] P.H. Lindenmeyer, Imperfections in polymer crystals, *Kolloid-Z. Z. Polym.* 231 (1) (1969) 593–605.
  - [45] J.H. Magill, Crystallization kinetics study of nylon 6, *Polymer* 3 (0) (1962) 655–664.
  - [46] P. Cebe, S.-D. Hong, Crystallization behaviour of poly(ether-ether-ketone), *Polymer* 27 (8) (1986) 1183–1192.
  - [47] K. Nakamura, T. Watanabe, K. Katayama, T. Amano, Some aspects of nonisothermal crystallization of polymers. I. Relationship between crystallization temperature, crystallinity, and cooling conditions, *J. Appl. Polym. Sci.* 16 (5) (1972) 1077–1091.
  - [48] K. Nakamura, K. Katayama, T. Amano, Some aspects of nonisothermal crystallization of polymers. II. Consideration of the isokinetic condition, *J. Appl. Polym. Sci.* 17 (4) (1973) 1031–1041.
  - [49] J.D. Hoffman, *Treatise on Solid State Chemistry*, Springer US, 1976.
  - [50] K.-H. Illers, H. Haberkorn, Schmelzverhalten, Struktur und Kristallinität von 6-Polyamid, *Makromol. Chem.* 142 (1) (1971) 31–67.
  - [51] I. Kolesov, D. Mileva, R. Androsch, C. Schick, Structure formation of polyamide 6 from the glassy state by fast scanning chip calorimetry, *Polymer* 52 (22) (2011) 5156–5165.
  - [52] C. Schick, V. Mathot, *Fast Scanning Calorimetry*, first ed., Springer International Publishing, 2016.
  - [53] C.N. Velisaris, J.C. Seferis, Crystallization kinetics of polyetheretherketone (PEEK) matrices, *Polym. Eng. Sci.* 26 (22) (1986) 1574–1581.
  - [54] P. Cebe, Application of the parallel avrami model to crystallization of poly(ether-etherketone), *Polym. Eng. Sci.* 28 (18) (1988) 1192–1197.
  - [55] J.J.E. Teuwen, *Thermoplastic Composite Wind Turbine Blades - Kinetics and Processability*, Thèse Technische Universiteit Delft, 2011.
  - [56] J. Merna, D. Chromcova, J. Brozek, J. Roda, Polymerization of lactams: 97. Anionic polymerization of  $\epsilon$ -caprolactam activated by esters, *Eur. Polym. J.* 42 (7) (2006) 1569–1580.
  - [57] P.W. Sibal, R.E. Camargo, C.W. Macosko, Designing nylon-6 polymerization systems for RIM, *Polym. Process Eng.* 1 (2) (1984) 147–169.
  - [58] N. Okui, S. Umamoto, R. Kawano, A. Mamun, Temperature and Molecular Weight Dependencies of Polymer Crystallization, Springer Berlin Heidelberg, Berlin, Heidelberg, 2007, pp. 391–425.
  - [59] B. Crist, J.M. Schultz, Polymer spherulites: a critical review, *Prog. Polym. Sci.* 56 (2016) 1–63.